Available online at www.sciencedirect.com
SCIENCE DIRECT®
Surface Science 532–535 (2003) 390–395
SURFACE SCIENCE
www.elsevier.com/locate/susc

High temperature postgrowing of Pt-nanocrystallites supported and encapsulated on $TiO_2(1\,1\,0)$ surface

A. Berkó *, J. Szökő, F. Solymosi

Institute of Solid State and Radiochemistry and the Reaction Kinetics Research Group of the Hungarian Academy of Sciences, University of Szeged, P.O. Box 168, H-6701 Szeged, Hungary

Abstract

High temperature postgrowing of Pt nanocrystallites is investigated on $TiO_2(1\,1\,0)$-$(1 \times n)$ support by scanning tunneling microscopy (STM). It was shown earlier for Rh and Ir that by growing the noble metal clusters at high temperature (1100 K), metal particle-arrays can be fabricated with desired average distances and narrow size-distributions [Surf. Sci. 400 (1998) 281; J. Catal. 182 (1999) 511]. In the case of Pt, Dulub et al. have recently reported an ordered and self-limiting $TiO_{1.1}$ overlayer grown on top of the supported metal nanoparticles on $TiO_2(1\,1\,0)$ [Phys. Rev. Lett. 84 (16) (2000) 3646]. It was shown in this work that the decoration with $TiO_{1.1}$ overlayer does not hinder the ordered growing of Pt nanocrystallites. The giant noble metal nanoparticles grown in large separation are suitable for further studies on their site selective reactivity and catalytic properties.

Keywords: Scanning tunneling microscopy; Scanning tunneling spectroscopies; Catalysis; Platinum; Titanium oxide

1. Introduction

Two dimensional model catalysts (2DMC) are more and more intensively used in today's heterogeneous catalytic research. This tendency is mainly due to the spreading application of scanning tunneling microscopy (STM), which resulted in a dramatic development in the characterization of nanoparticles supported on oxide surfaces [1–3]. The studies of 2DMC systems have obviously opened new paths to obtain deeper insight into some pristine phenomena of heterogenous catalysis, for example the strong metal–support interaction (SMSI) or the so-called decoration process.

The decoration layer formed on top of the metal nanoparticles supported on reducible oxides may play a crucial role in fine tuning the performance of the oxide supported catalysts. Accordingly, a great effort has been made recently to understand this phenomenon on the atomic scale [4–6]. Two important processes are involved in the formation of SMSI state: (1) a surface diffusion of atoms or few atomic species from the reduced support to the top of the metal nanoparticles; (2) formation of strained ultrathin decoration film on the crystallite of limited area. The kinetics of the former process can be experimentally studied by video-STM providing certainly very interesting results in the near future. To understand the latter process, i.e. the ordering of the decoration layer, it is sufficient to apply a conventional static STM, although specially grown metal nanoparticles of

* Corresponding author. Fax: +36-68-424-997.
E-mail address: aberko@chem.u-szeged.hu (A. Berkó).

0039-6028/03/$ - see front matter
doi:10.1016/S0039-6028(03)00146-8

very large size (<10 nm) are needed to obtain high quality STM images [5,6]. Recent works demonstrated that a well ordered, polar and self-limiting oxide double layer of O:Ti = 1.1 stoichiometry is formed on the (1 1 1) oriented top facets of Pt nanocrystallites supported on a TiO_2(1 1 0) surface [6]. We may assume that in the ordering of the overlayer the size of the decorated particle plays a decisive role. This feature presses for the development of an applicable method for growing well separated and very large particles. The "seeding and growing" method developed in our laboratory seems to be a very suitable procedure for this purpose; we have fabricated Ir and Rh nanocrystallites of very narrow size-distribution on a TiO_2(1 1 0)-(1 × 2) support [7–9]. It is not clear yet, whether the second step of this fabrication process ("growing at high temperatures") results in decorated or undecorated nanocrystallites. In the case of Pt it is very likely that metal particles grown at high temperatures will be decorated. In this way the main question is how does the encapsulating layer influence the growing of the particles.

In this work a TiO_2(1 1 0)-(1 × n) surface is seeded with Pt crystallites by the deposition of metal in a few tenth of monolayer (ML) coverage at 300 K followed by annealing at 1100 K in UHV; the Pt seeds (average diameter 2–3 nm) so formed were step by step grown further at 1100 K into very large crystallites (20–30 nm). The distribution and shape of the crystallites, moreover, their decoration with TiO_x layer are investigated by scanning tunneling microscopy (STM) and spectroscopy (STS) methods.

2. Experimental

The experiments were carried out in an UHV chamber equipped with a commercial room temperature STM-head, an electron energy analyzer (RFA) for AES and a quadrupole mass spectrometer for gas analysis. The polished TiO_2(1 1 0) single crystal sample of 7 × 5 × 1 mm^3 was purchased from PI-KEM (UK). It was clipped on a Ta-plate and heated by a W-filament from the rear side. The temperature was measured by K-type (chromel–alumel) thermocouple sticked to the side of the sample by ceramobond 503 (AREMCO). The cleaning procedure consisted of annealing at 900 K in UHV for a few days, several cycles of Ar^+ sputtering (1.5 keV, 10^{-6} A/cm^2, 10 min) and postannealing for a few minutes at 1200 K. The samples were moved with an UHV-compatible transfer system from the STM-head to the central manipulator where the different treatments of the sample were performed. A side vacuum chamber served for changing the probe and for treatment in gases at high pressures. The complete system was evacuated by ion-getter and turbomolecular pumps in order to achieve an ultimate pressure of 5×10^{-10} mbar.

Pt was deposited by resistive heating of a high purity (99.95%) Pt filament. The rate of the evaporation was controlled by adjusting the filament current. The cleanness of the sample surface and the ultrathin metal adlayer was checked by Auger electron spectroscopy. The Pt coverage is expressed in monolayer (ML) equivalent which corresponds to 1.6×10^{15} atom/cm^2. The actual coverage was calculated by the determination of the total volume of the well separated 3D metal nanoparticles formed on the effect of annealing at 1100 K and by taking into account the atom density of Pt. It should be remarked that this method may contain some systematic error because of encapsulation or/and sinking of the supported nanoparticles; nevertheless these effects may cause an error less than 20–30% in our case.

For STM imaging, chemically edged W tips were applied and sharpened "in situ" above the TiO_2 surface by applying 5–10 V pulses. Tunneling parameters of +1.5 V bias voltage and 0.2 nA tunneling current were typically used for imaging. The STM pictures consisting of 256 × 256 points were collected within 1–3 min depending on the corrugation of the surface. The characteristic images shown in this work were chosen from numerous records obtained on different regions of the sample.

3. Results and discussion

3.1. Characterization of the TiO_2(1 1 0)-(1 × n) surface

The clean TiO_2(1 1 0) surface used as a support in this work exhibited characteristic added rows

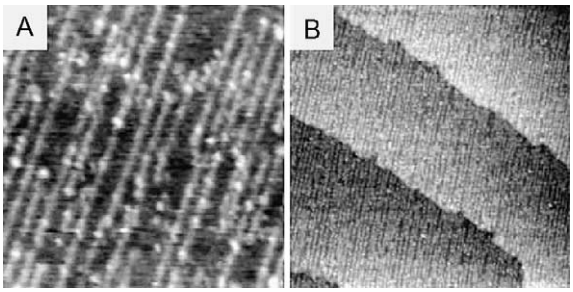

Fig. 1. Characteristic STM images recorded on the clean $TiO_2(1\,1\,0)$-$(1 \times n)$ substrate for two different image sizes: (A) 50 nm × 50 nm; (B) 200 nm × 200 nm.

running in the [0 0 1] crystallographic orientation. This morphology can be seen in Fig. 1 for two different image sizes. The sizes of the terraces are apparently rather large (typically 80 nm × 200 nm) and the characteristic steps run in the [1 1 1] direction. This morphology clearly suggests that the accuracy of the orientation of the sample is better than 0.2°. The surface density of the 1D structures largely depends on the duration of the annealing at 1100 K. In these experiments the ordering of the surface sputtered by Ar^+ typically lasted for 10 min. An average periodicity of 1.95 and 2.60 nm was measured perpendicularly to the outrising rows which means (1×3) or (1×4) reconstruction of the surface. It is worth mentioning that in the case of other $TiO_2(1\,1\,0)$ single crystals used in our laboratory the same treatments resulted in mainly (1×2) surface structure with an average terrace size of 15 nm × 30 nm [10]. Comparing the characteristic surface structures of $TiO_2(1\,1\,0)$ published recently by different laboratories, it can be stated that basically just these two different morphologies are reported for that material [11–15] (not listing all these papers). Looking for the explanation of this feature, it has to be kept in mind that the average sizes of the terraces always exhibit a correlation with the 1D row morphology: the smaller the terraces, the higher the probability for a total (1×2) reconstruction.

3.2. Postgrowing of Pt nanoparticles formed on $TiO_2(1\,1\,0)$-$(1 \times n)$ surface at 1100 K

Fig. 2A shows the characteristic morphology of a $TiO_2(1\,1\,0)$-$(1 \times n)$ surface imaged after the

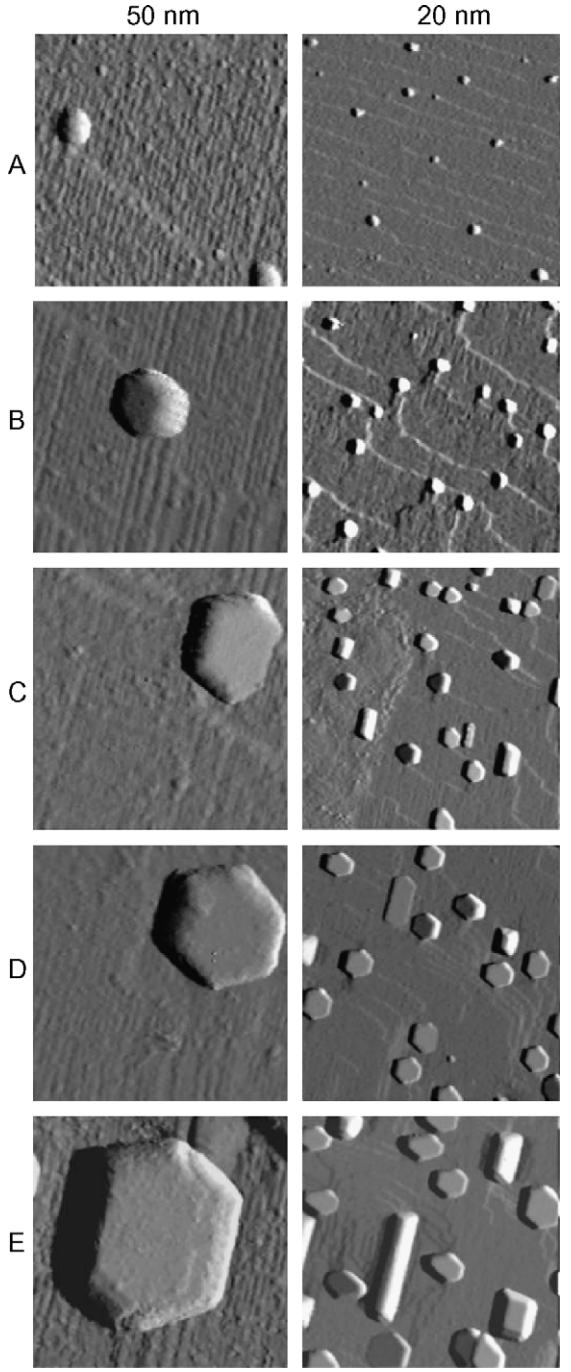

Fig. 2. STM images of two different sizes for the stepwisely grown Pt seeds formed by deposition of 0.01 ML of Pt at 300 K followed by annealing for 10 min at 1100 K. (A) Pt seeds; deposition of further Pt upto (B) 0.25 ML; (C) 0.56 ML; (D) 1.28 ML; (E) 2.80 ML coverages at 1100 K.

deposition of 0.01 ML Pt at 300 K followed by annealing at 1100 K for 10 min (''seeding''). In this case a single particle in average can be detected on an area of 50 nm × 50 nm. At lower magnification (200 nm × 200 nm) it can be seen that the particles are distributed rather uniformly, although the average diameter of the crystallites shows a variation in the range of 2–4 nm. Supported Pt-particles are located at the steps or, more exactly, at the cross points of two different steps. It is worth mentioning that the surface concentration of the seeds can be varied by fine tuning the amount of the deposited metal. In harmony with our earlier observation [8], the surface density of the nanoparticles (seeds) increases almost linearly with the metal coverage in the range of 0.001–0.050 ML. The second part of the nanofabrication procedure is the postgrowing of Pt-particles by the evaporation of further amounts of Pt at 1100 K (Fig. 2B–E). The main feature is that the average size of the metal particles increases gradually from 2–4 nm upto 20–30 nm without the formation of new ones. As was experimentally proved (not presented here) Pt-particles do not evaporate from the surface at 1100 K, in this way, the deposited amount of the metal (listed in the legend of the figure) can be calculated from the total volume of the particles. With the exception of the highest total coverage (2.80 ML), the size-distribution of the particles is rather narrow, the shape of the particles is also very similar and all of them are oriented with one side along the [0 0 1] direction of the support. The nanocrystallites exhibit mostly (≈80%) a hexagonal outline with flat (1 1 1) top facets declined by 5–6° to the terrace plane of the support, at the same time some particles are strongly elongated in the surface orientation of [0 0 1] or they exhibit a square (1 0 0) top facet. It is worth mentioning here that in the case of Rh and Ir the same growing procedure has resulted in rather elongated crystallites which can be explained by the lower melting point of Pt. The largest crystallites contain approximately 20–30 Pt-layers. STM images and the tunneling spectra recorded on the top of the crystallites have shown the formation of an ordered insulator character overlayer which will be discussed below. Summing up these results, we may conclude that the ''seeding + growing'' method results in taylored distribution and in an ordered inner structure of Pt crystallites postgrown on the $TiO_2(1\,1\,0)$-$(1 \times n)$ surface. A more detailed analysis of the mechanism of formation and postgrowing of noble metal nanoparticles can be find in our earlier works [7,8].

3.3. Tunneling microscopy and spectroscopy characterization of ordered TiO_x layer formed on top of the postgrown Pt crystallites

The formation of ordered decoration layer can be detected by STM only for the largest crystallites which have a flat top facet. In Fig. 3A a Pt crystallite of 40 nm long and 30 nm wide can be seen on the STM image of 50 nm × 50 nm. The height of the crystallite is approximately 4 nm, which means 16–18 parallel Pt layers of (1 1 1) indexes in the particle. The top facet is declined to the plane of the support by approximately 6°. The high resolution images recorded on the upper facet of the crystallite are shown for two different tunneling biases: (B) +1.5 V; (C) −1.0 V. Although the stability of our equipment does not make it possible to obtain as good quality images as Dulub and co-workers [5,6], nevertheless it can be seen clearly that for a positive bias, periodic rows are running in the diagonal direction of the picture (Fig. 3B). These rows are parallel to one side of the Pt crystallite and the average periodicity is 1.6 nm. This value is the same as the distance of the ''zigzag'' stripes suggested in the model for the ordered decoration layer by Dulub and co-workers [6]. For negative bias, a rather different structure can be seen in Fig. 3C which can be explained by the electronic sensitivity of the imaging of overlayer. In harmony with the former findings, the hexagonally ordered light patches can be identified as neighbouring surface oxygen atoms in the decorating overlayer. The average distance between these patches is 1.9 nm, corresponding well to the model given by Dulub and co-workers [5,6]. The existence of a $TiO_{1.1}$ decorating layer is also supported by the tunneling spectroscopy measurements. The I–V curve above the central point of the crystallite is drawn in Fig. 3D. The almost zero slope at the Fermi level and the ''wide gap'' character of the curve refer clearly to a

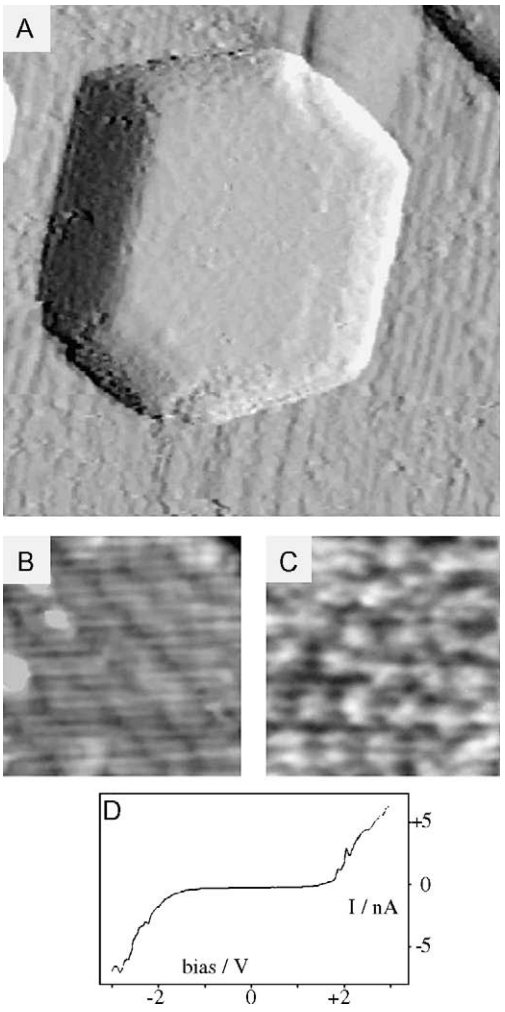

Fig. 3. Characterization of the decoration overlayer formed on the large hexagonal Pt crystallites by tunneling microscopy and spectroscopy. (A) An individual hexagonal Pt crystallite formed in the postgrowing process. (B) and (C) STM images recorded on the top facets of the previous crystallite for two different tunneling voltages: +1.5 and −1.0 V, respectively. (D) A wide range *I–V* spectra taken up on the top facet of the crystallite shown in (A).

non-metallic behaviour of the upper facet of the crystallite. It should be mentioned that after a slight Ar^+ bombardment this property changes to a behaviour of metallic character. On the basis of the presented experimental results in this section we may conclude that the encapsulating $TiO_{1.1}$ overlayer does not apparently influence the post-growing procedure applied for the fabrication of giant and well separated noble metal crystallites. The temperature (1100 K) applied for the post-growing is seemingly not sufficient for activation of the de-encapsulation of Pt-particles in our case, although this latter process was readily observed in several cases [16,17].

4. Conclusions

The "seeding and growing" method was applied in this work for growing Pt crystallites in predetermined surface concentration and average size on the $TiO_2(1\,1\,0)$-$(1 \times n)$ substrate. It was demonstrated that in spite of an ordered decorating TiO_x layer formed on the top of Pt nanocrystallites supported on $TiO_2(1\,1\,0)$-$(1 \times n)$ surface, they can be postgrown of high inner ordering at 1100 K.

Acknowledgements

The authors gratefully acknowledge the support of the Hungarian Scientific Research Fund through T29952, TS40877 and T32040 projects. The authors also express their thanks to Miss Orsolya Hakkel for her valuable assistance.

References

[1] C.T. Campbell, Surf. Sci. Rep. 27 (1–3) (1997) 1.
[2] C.R. Henry, Surf. Sci. Rep. 31 (1998) 231.
[3] M. Bäumer, H.-J. Freund, Prog. Surf. Sci. 61 (1999) 127.
[4] A. Berkó, I. Ulrych, K.C. Prince, J. Phys. Chem. B 102 (1998) 3379.
[5] O. Dulub, W. Hebenstreit, U. Diebold, Phys. Rev. Lett. 84 (16) (2000) 3646.
[6] D.R. Jennison, O. Dulub, W. Hebenstreit, U. Diebold, Surf. Sci. 492 (2001) L677.
[7] A. Berkó, F. Solymosi, Surf. Sci. 400 (1998) 281.
[8] A. Berkó, G. Klivényi, F. Solymosi, J. Catal. 182 (1999) 511.
[9] A. Berkó, J. Szökő, F. Solymosi, Solid State Ionics 141–142 (2001) 197.
[10] A. Berkó, F. Solymosi, Surf. Sci. 411 (1998) L900.
[11] H. Onishi, Y. Iwasawa, Surf. Sci. 313 (1994) L783.
[12] S. Fischer, A.W. Munz, K.-D. Schierbaum, W. Göpel, J. Vac. Sci. Technol. B 14 (2) (1996) 961.
[13] I.D. Cocks, Q. Guo, E.M. Williams, Surf. Sci. 390 (1997) 119.

[14] R.A. Bennett, S. Poulston, P. Stone, M. Bowker, Phys. Rev. B 59 (1999) 10341.
[15] M. Li, W. Hebenstreit, U. Diebold, Phys. Rev. B 61 (7) (2000) 4926.
[16] A. Berkó, G. Ménesi, F. Solymosi, Surf. Sci. 372 (1996) 202.
[17] S. Ko, R.J. Gorte, J. Catal. 90 (1984) 59; Surf. Sci. 161 (1985) 597.